



ELSEVIER

16 December 1996

PHYSICS LETTERS A

Physics Letters A 223 (1996) 394–399

Thin films of a binary polymer mixture: calculations of the concentration profile for asymmetric walls

C.D. Eggleton

Department of Biomedical Engineering, Johns Hopkins School of Medicine, 720 Rutland Avenue, Baltimore, MD 21205, USA

Received 13 May 1996; revised manuscript received 23 September 1996; accepted for publication 25 September 1996

Communicated by L.J. Sham

Abstract

A numerical method for studying equilibrium behavior of thin films between symmetric and asymmetric walls using mean field theory is described. Calculated critical lengths for phase separation between symmetric walls increase as the effective wall composition deviates from the average concentration. Concentration profiles between asymmetric walls are presented.

PACS: Thin film; Polymer mixture; Phase transition; Asymmetric walls; Surface enrichment

1. Introduction

In the past 10 years, there has been a great interest in the surface properties of polymer blends. The use of experimental techniques such as neutron reflectivity [1] and nuclear reaction analysis [2] allows the details of the near-surface concentration profile to be measured. These techniques are now being applied to thin films [2]. The first theories to predict the concentration profile for mixtures in thin films was developed by Jerry and Nauman [3] and Parry and Evans [4]. Mass conservation is enforced in the first theory but not in the latter. Mass conservation does not need to be considered when studying the magnetic properties of thin films. A similar approach for the cases when mass conservation is enforced was used by Tang [5].

Recently, Flebbe et al. [6] have studied the case of a binary polymer mixture between symmetric walls. They have shown that the lowest free energy (equilibrium) concentration profile is not one dimensional. Instead, the binary mixture separates to form

two “phases” with the interface running orthogonal to the walls. The concentration profile approaches a one-dimensional structure at a large distance from the interface. On the other side of the interface a different one-dimensional structure is attained. Bruder and Brenn [7] conducted experiments which started with a monolayer of uniform composition. After annealing, they obtained a laterally homogeneous structure that could be modeled with Jerry and Nauman theory. The Flebbe 2-phase theory however would be more appropriate for experiments such as those of Straub [8] that start with a monolayer but after annealing, obtained a laterally inhomogeneous structure. A laterally inhomogeneous structure was also obtained after annealing in the experiments of Steiner [9], who started with a two-layer initial phase distribution. Both the Jerry and Nauman one-dimensional profile, and the Flebbe laterally inhomogeneous structure have been observed in experiments. Thus, both theoretical modeling efforts are appropriate under different experimental conditions.

In this paper, we present a numerical approach to find one-dimensional concentrations profiles when the two walls and degree of polymerization are different. Mass conservation is included in the governing equations and the average concentration of the profile can be fixed. It is important to recognize that these metastable states may not be the lowest free energy state, which can only be determined through three-dimensional simulations.

2. Theory

The mean field free energy for mixtures between two parallel walls as proposed by Cahn [10] is represented by

$$F = \int_0^L \left[f(s) + \frac{\kappa}{2} \left(\frac{ds}{dx} \right)^2 + \lambda (s - \bar{s}) \right] dx + \Phi_\ell(s_\ell) + \Phi_r(s_r). \quad (1)$$

The dimensionless free energy density of mixing of polymer A and B having degrees of polymerization N_1 and N_2 , respectively, is given by

$$f(s) = \frac{1}{N_1} s \ln(s) + \frac{1}{N_2} (1-s) \ln(1-s) + \chi s(1-s), \quad (2)$$

where s is the volume fraction of polymer A, χ is the Flory interaction parameter, L is the wall separation, x is the depth into the film, κ is the gradient energy parameter, and Φ is the surface energy contribution. The subscript ℓ refers to the left boundary which is located at $x = 0$, and r to the right one at $x = L$. In the present analysis, it is assumed that the concentration profile is a one-dimensional function of x alone. The differential equation for the equilibrium concentration profile is given by setting the variational derivative of Eq. (1) equal to zero, yielding

$$\frac{df}{ds} + \frac{1}{2} \frac{d\kappa(s)}{ds} \left(\frac{ds}{dx} \right)^2 - \frac{d}{dx} \left(\kappa(s) \frac{ds}{dx} \right) + \lambda = 0 \quad (3)$$

with the corresponding expression for the second derivative of the concentration profile:

$$\frac{d^2s}{dx^2} = \frac{1}{\kappa(s)} \left[\frac{df}{ds} - \frac{d}{ds} \frac{\kappa(s)}{2} \left(\frac{ds}{dx} \right)^2 + \lambda \right], \quad (4)$$

where $\kappa(s)$ is given by

$$\kappa(s) = \frac{a^2}{18s(1-s)} \quad (5)$$

and boundary conditions at the walls

$$\frac{ds}{dx_\ell} = \frac{1}{\kappa(s_\ell)} \frac{\partial \Phi_\ell(s_\ell)}{\partial s}, \quad (6)$$

$$\frac{ds}{dx_r} = -\frac{1}{\kappa(s_r)} \frac{\partial \Phi_r(s_r)}{\partial s}. \quad (7)$$

The $\Phi_\ell(s)$ and $\Phi_r(s)$ functions are typically taken to be a quadratic [11],

$$\Phi_\ell(s) = -\mu_\ell s - \frac{1}{2} g_\ell s^2, \quad (8)$$

$$\Phi_r(s) = -\mu_r s - \frac{1}{2} g_r s^2, \quad (9)$$

where the coefficients μ_1 and g are properties of the mixture itself and of the walls [11]. The more conventional parameters μ_1 and g are related to M , which depends only on the mixture, and the effective wall composition, w , that depends on mixture and wall properties [3] through

$$\mu_1 = M\chi w, \quad (10)$$

$$g = -M\chi. \quad (11)$$

The equation for the conservation of mass,

$$\int_0^L s(x) dx = \bar{s}L, \quad (12)$$

is needed to evaluate the Lagrange multiplier, λ , and for consistency.

3. Numerical solution of the concentration profile

The shooting method has been used by Flebbe, Dunweg and Binder (FDB) and Parry and Evans to find thin film concentration profiles between symmetric and arbitrary (symmetric and asymmetric) bounding walls, respectively. Assuming a symmetric profile, the slope at the centerline is known to be zero while the

concentration is unknown. In the case of asymmetric bounding walls the slope is dependent on the assumed concentration. Varying the centerline/wall concentration s_0 from 0 to 1, Eq. (4) is integrated and yields a family of profiles. The correct profile is determined by satisfying the boundary conditions at the second bounding surface. The average concentration of the profile will depend on the value of the Lagrange multiplier chosen for Eq. (4). The Lagrange multiplier must be varied until the value which gives the desired average concentration is found. A numerical method for finding the concentration profile for asymmetric properties of the bounding surfaces and polymer mixture which enforces mass conservation is described in this section. Variations of the concentration at the walls and the Lagrange multiplier are not required to find a solution which satisfies the boundary condition and has the desired average concentration. The solution obtained depends on the initial profile and is a metastable state, but is not necessarily to be the lowest free energy state. Different initial conditions are used and the free energy of the metastable solutions found must be calculated.

The equilibrium concentration profile is found by discretizing the governing equations. The film thickness is discretized into a grid with N nodes and standard finite difference approximations yields an algebraic equation for the free energy at an interior node i :

$$\begin{aligned} \frac{df}{ds_i} + \frac{1}{2} \frac{d\kappa(s_i)}{ds} \left(\frac{s_{i+1} - s_{i-1}}{\Delta x} \right)^2 \\ - \frac{1}{\Delta x} \left(\frac{\kappa_{i+1/2}(s_{i+1} - s_i)}{\Delta x} - \frac{\kappa_{i-1/2}(s_i - s_{i-1})}{\Delta x} \right) \\ + \lambda = 0, \end{aligned} \quad (13)$$

where

$$\kappa_{i+1/2} = \frac{1}{2} [\kappa(s_{i+1}) + \kappa(s_i)] \quad (14)$$

with boundary conditions

$$\frac{s_2 - s_1}{\Delta x} = \frac{M\chi}{\kappa(s_1)}(s_1 - w), \quad (15)$$

$$\frac{s_N - s_{N-1}}{\Delta x} = -\frac{M\chi}{\kappa(s_N)}(s_N - w). \quad (16)$$

The trapezoidal rule for integration is used to evaluate Eq. (12),

$$\frac{1}{2}s_1 + s_2 + s_3 + \dots + s_{N-2} + s_{N-1} + \frac{1}{2}s_N. \quad (17)$$

A Newton–Raphson iterative procedure is used to find the discrete equilibrium concentration and Lagrange multiplier given by

$$\mathbf{u} = [s_1, s_2, \dots, s_{N-1}, s_N, \lambda] \quad (18)$$

starting from an initial profile and Lagrange multiplier. The change in the unknown quantities at iteration n , $\Delta \mathbf{u}^n$, is found by solving the system of $N+1$ algebraic equations

$$\frac{\partial \mathbf{R}^n}{\partial \mathbf{u}^n} \cdot \Delta \mathbf{u}^n = -\mathbf{R}^n \quad (19)$$

where

$$\Delta \mathbf{u}^n = [\Delta s_1, \Delta s_2, \dots, \Delta s_{N-1}, \Delta s_N, \Delta \lambda], \quad (20)$$

$$\mathbf{R}^n = [R_1, R_2, \dots, R_i, \dots, R_{N-1}, R_N, R_{N+1}], \quad (21)$$

$$R_1 = \frac{s_2 - s_1}{\Delta x} - \frac{M\chi}{\kappa(s_\ell)}(s_1 - w), \quad (22)$$

$$\begin{aligned} R_2 = \frac{df}{ds_2} + \frac{1}{2} \frac{d\kappa(s_2)}{ds} \left(\frac{s_3 - s_1}{\Delta x} \right)^2 \\ - \frac{1}{\Delta x} \left(\frac{\kappa_{2+1/2}(s_3 - s_2)}{\Delta x} - \frac{\kappa_{2-1/2}(s_2 - s_1)}{\Delta x} \right) \\ + \lambda, \end{aligned} \quad (23)$$

$$\begin{aligned} R_i = \frac{df}{ds_i} + \frac{1}{2} \frac{d\kappa(s_i)}{ds} \left(\frac{s_{i+1} - s_{i-1}}{\Delta x} \right)^2 \\ - \frac{1}{\Delta x} \left(\frac{\kappa_{i+1/2}(s_{i+1} - s_i)}{\Delta x} - \frac{\kappa_{i-1/2}(s_i - s_{i-1})}{\Delta x} \right) \\ + \lambda, \end{aligned} \quad (24)$$

$$\begin{aligned} R_{N-1} = \frac{df}{ds_{N-1}} + \frac{1}{2} \frac{d\kappa(s_{N-1})}{ds} \left(\frac{s_N - s_{N-2}}{\Delta x} \right)^2 \\ - \frac{1}{\Delta x} \left(\frac{\kappa_{N-1/2}(s_N - s_{N-1})}{\Delta x} - \frac{\kappa_{N-3/2}(s_{N-1} - s_{N-2})}{\Delta x} \right) \\ + \lambda, \end{aligned} \quad (25)$$

$$R_N = \frac{s_N - s_{N-1}}{\Delta x} + \frac{M\chi}{\kappa(s_\ell)}(s_N - w), \quad (26)$$

$$R_{N+1} = \frac{1}{2}s_1 + s_2 + s_3 + \dots + s_{N-2} + s_{N-1} + \frac{1}{2}s_N. \quad (27)$$

The matrix $\partial R/\partial u$ is found by taking the derivative of each component of R_i with respect to each u_i . This results in a bordered linear system of the form

$$\begin{bmatrix} A & B \\ C & D \end{bmatrix} \cdot \begin{bmatrix} \Delta s_i \\ \Delta \lambda \end{bmatrix} = - [R_i]. \quad (28)$$

Here, A is tridiagonal matrix given by $\partial R_i/\partial s_i$. Each element of the $N \times 1$ vector B is 1 and is due to the appearance of λ in Eq. (13). The elements of the $1 \times N$ vector C come from the coefficients of s_i in Eq. (17) for mass conservation. The scalar D is zero. Solutions to systems of this form can be found efficiently using the block elimination method [12]. There are films, such as magnetic films, where mass conservation is not applicable. In these situations the mass conservation equation Eq. (12) is removed from the system, and the value of λ is found independently. The resulting system of equations is tridiagonal and can be solved efficiently using Thompson’s algorithm [13].

Solving the discretized system of equations gives Δu . A relaxation parameter α is used to adjust the magnitude of the correction, such that the new vector of unknowns u^{n+1} is given by

$$u^{n+1} = u^n + \alpha \Delta u^n. \quad (29)$$

Iterations are continued until the largest element of Δu_i is less than 10^{-12} .

4. Symmetric concentration profiles

The advantage of the proposed numerical method is that values of the concentration and its gradient at the bounding wall, nor the value of the Lagrange multiplier that determines the average concentration of the profile need to be specified. The metastable profile to which the method converges depends on the initial concentration profile. First, profiles are found for symmetric bounding walls and the solutions are compared with those obtained integrating Eq. (4) in the manner described by FDB in order to validate the new method.

The following parameters are used: $N_1 = N_2 = 100$, $\chi = 0.026$, $w = 0.4$, $M_\ell = 0$, and $M_r = 19.23077$, which correspond to those used in Fig. 5b of FDB. The solutions found for the symmetric boundaries were found for fixed λ and allowed \bar{s} to vary. Eq. (12) en-

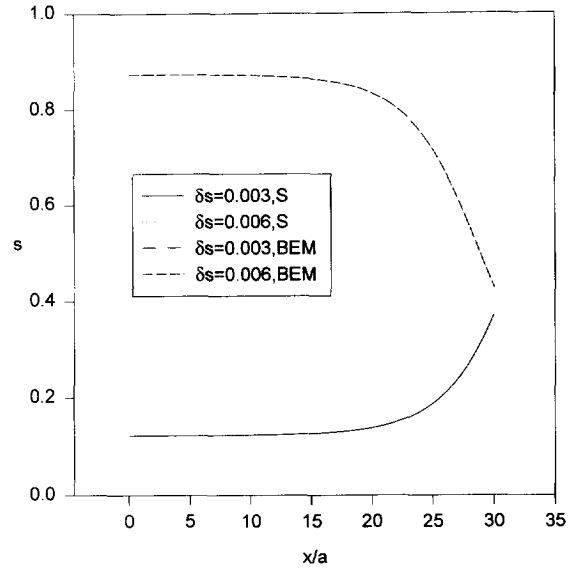


Fig. 1. Concentration profiles for symmetric walls. Solution of the governing ODE using the shooting method (S) is compared with the newly proposed method using the block elimination method (BEM). The largest error is 0.037% for $\delta s = 0.003$ and 0.08% for $\delta s = 0.006$.

forcing mass conservation is removed from the system. The fixed value of λ is related to the parameters of the symmetric calculations of FDB through

$$\lambda = - \left[\frac{1}{N} \ln \left(\frac{s_b}{1 - s_b} \right) + \chi(1 - 2s_b) \right]. \quad (30)$$

The concentration s_b is obtained from

$$s_b = \delta s + s_{co2}, \quad (31)$$

where δs is the parameter used by FDB, and s_{co2} is the larger of the binodal concentrations.

Here, the concentration dependence of κ is included and lengths are nondimensionalized by the effective lattice spacing a . The nondimensional half width of the film is fixed at 30. Concentration profiles shown for half of the film between symmetric walls in Fig. 1 using our method are in very good agreement with those calculated using the FDB integral method. The difference in the solutions found on discretized film thickness with one hundred nodes ($\Delta x = L/100$) are greatest at the wall and are 0.15% and 0.08% for $\delta s = 0.003$ and $\delta s = 0.006$, respectively. It was found that this level of discretization resulted in a slight error that

was visible when compared to the solution for the integral method at $\delta s = 0.003$. A grid refinement study was done and it was found that for $(\Delta x = L/400)$ the error was reduced to 0.037%. This solution is shown in Fig. 1. Numerical difficulties were encountered by FDB in regions where the concentration profile is rather flat, because the integrand of the shooting method becomes singular. The present method did not encounter such difficulties in the flat regions of the curves in Fig. 1 since the partial differential equation is being approximated. In these flat regions, approximations of the derivatives approach zero and cause no numerical instabilities.

5. Critical length for phase transition in symmetrically bounded films

A theory by Jerry and Naumann [3] gives an expression for the critical length, \tilde{L}_c ,

$$P\tilde{L}_c = \arccos\left(\frac{(M\chi/P)^2 - 1}{(M\chi/P)^2 + 1}\right), \quad (32)$$

where

$$P^2 = -\frac{d^2 f(\bar{s})}{ds^2}. \quad (33)$$

This expression was shown to be valid only when \bar{s} is close to w . Here, the behavior of \tilde{L}_c for extreme values of w is determined.

The numerical method is used to study how the critical length depends on the wall concentration w . In this section it is assumed that κ is not concentration dependent in order to compare with linear theory. Both the theory and the calculations assume lateral homogeneity, making the governing equations one dimensional and excluding the possibility of lateral inhomogeneities. The critical length is determined using a continuation procedure. A film thickness larger than the expected critical length is chosen and the phase separated equilibrium profile is found. This profile is then scaled for a smaller film thickness L_d , and used as the initial condition for finding the profile over L_d . If the equilibrium profile obtained is symmetric and has only one maximum/minimum or is flat, it corresponds to the unseparated profile. In this case, a smaller value of ΔL (the difference in the film thickness for the initial condition and the new thickness) is used until a

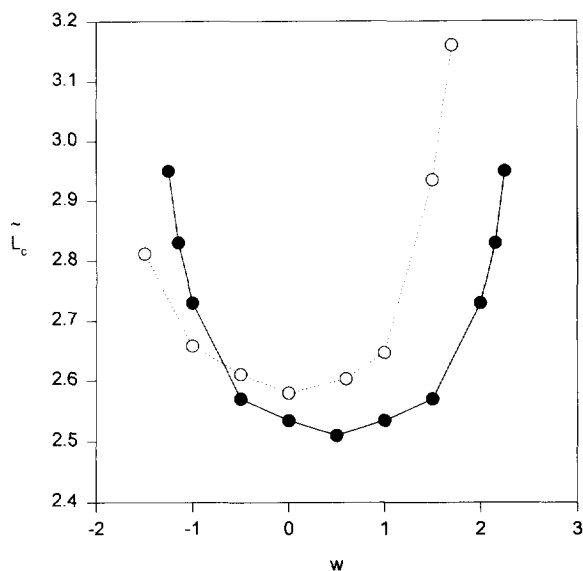


Fig. 2. Dependence of critical length for phase transition between symmetric walls on wall mole fraction w . Calculated \tilde{L}_c for the following physical parameters: $N_1 = N_2 = 1$, $\chi = 3$, $M_\ell = M_r = 0.1$; $\bar{s} = 0.5$ (\bullet) and $\bar{s} = 0.6$ (\circ).

phase separated profile is obtained. The continuation procedure is stopped when $\Delta L/L_d < 10^{-2}$. The free energy of the film is also calculated, and at the critical film thickness the energies of the phase separated and mixed films are equal.

Critical length is shown as a function of the wall concentration profile w , in Fig. 2 for $N_1 = N_2 = 1$, $\bar{s} = 0.5$, $M = 0.1$, and $\chi = 3$. Lines are used to connect the calculated points to aid in following the trends in \tilde{L}_c . Here, lengths are nondimensionalized by $\kappa^{1/2}$. The nonlinear numerical method gives $\tilde{L}_c = 2.55$ for $w = \bar{s}$ and agrees with the analytic prediction of linear theory. Note that the calculated \tilde{L}_c are always greater than or equal to the Jerry and Naumann value. Also, for $\bar{s} = 0.5$ the value of \tilde{L}_c is symmetric about $w = 0.5$ and rises sharply as the magnitude of w increases. For the case $\bar{s} = 0.6$, \tilde{L}_c increases more sharply when $w > \bar{s}$. Thus, if the walls are properly selected with a sufficiently large value of w , it would be possible to prepare nearly uniform thin films of polymer mixtures that would be incompatible in bulk.

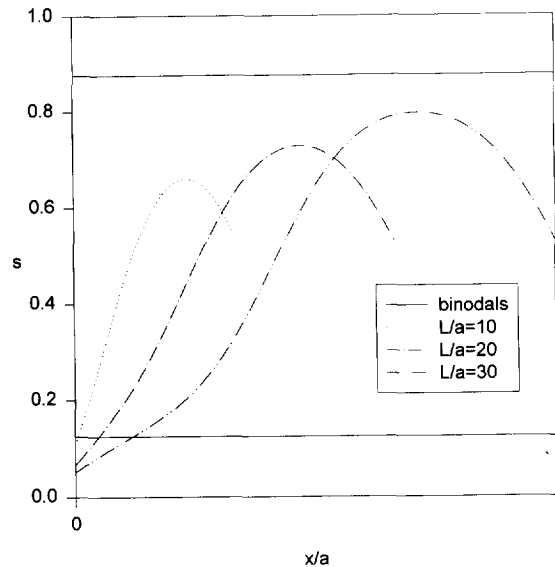


Fig. 3. Concentration profiles for asymmetric walls $\bar{L} = 10\text{--}30$. Calculated profiles for $N_1 = N_2 = 100$, $\chi = 0.026$, $M_\ell = 0$, $M_r = 19.2073$, $w_\ell = 0$, $w_r = 0.5$, $\bar{s} = 0.5$.

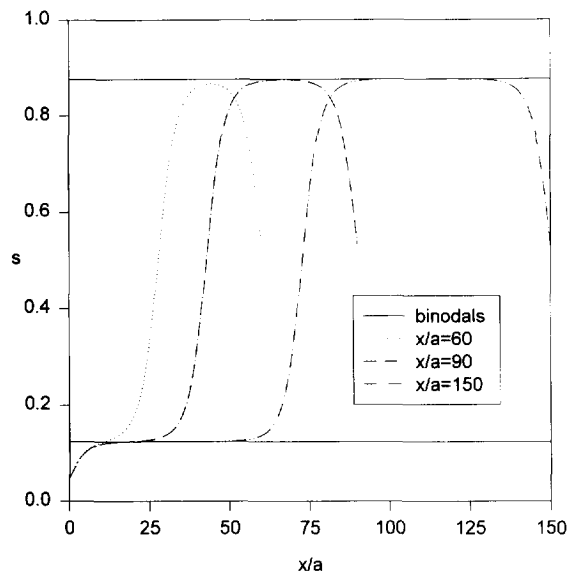


Fig. 4. Concentration profiles for asymmetric walls $\bar{L} = 60\text{--}150$ (same parameters as in Fig. 3).

6. Thin films bounded by asymmetric walls

The advantage of the proposed numerical method is that the magnitudes of the concentration and its gradient at the boundaries can be left unspecified. In

this case the physical parameters used are $N_1 = N_2 = 100$, $\bar{s} = 0.5$, $w_\ell = 0$, $w_r = 0.5$, $M_\ell = M_r = 19.20377$. The film thickness is nondimensionalized by the effective lattice spacing, a , and increased.

The concentration profiles calculated using the proposed numerical technique are shown in Figs. 3 and 4. For the case of asymmetric walls, the one-dimensional profile may not be the lowest free energy state according to theory of FDB. However, these profiles should be observed in experiments such as those reported by Budkowski [14–16], in which the films are prepared by attaching together two films of different polymer components and annealing. Budkowski and coworkers [14] were not able to calculate their observed profiles in an a priori fashion. The calculated profiles depended on the bulk plateau concentration and the solid surface concentration measured for each profile. Their measurements show that the concentration profile across thin films of binary polymer mixtures are dependent on film thickness and wall interactions. The numerical method proposed can be used to predict these variations in an a priori fashion.

References

- [1] R.J. Composto, R.S. Stein, G.P. Felcher, A. Mansour and A. Karim, *Physica B* 156–157 (1989) 434.
- [2] U. Chaturvedi, U. Steiner, O. Zak, G. Krausch, G. Schatz and J. Klien, *Appl. Phys. Lett.* 56 (1990) 1228.
- [3] R. Jerry and E. Nauman, *Phys. Lett. A* 167 (1992) 198.
- [4] A.O. Parry and R. Evans, *Physica A* 181 (1992) 250.
- [5] H. Tang, I. Szleifer and S.K. Kumar, *J. Chem. Phys.* 100 (1994) 5367.
- [6] T. Flebbe, B. Dunweg and K. Binder, *J. Phys. II (Paris)* 6 (1996) 667.
- [7] F. Bruder and R. Brenn, *Phys. Rev. Lett.* 69 (1992) 624.
- [8] W. Straub, F. Bruder, R. Brenn, G. Krausch, H. Bielefeldt, A. Kirsch, O. Marti, J. Mlynek and J. Marko, *Europhys. Lett.* 29 (1995) 353.
- [9] U. Steiner, J. Klein and L.J. Fetters, *Phys. Rev. Lett.* 72 (1994) 1498.
- [10] J.W. Cahn, *J. Chem. Phys.* 66 (1977) 3667.
- [11] I. Schmidt and K. Binder, *J. Phys. (Paris)* 46 (1985) 1631.
- [12] W. Govaerts and J. Pryce, *IMA J. Num. Anal.* 13 (1993) 161.
- [13] C. Hirsh (Wiley, New York, 1988).
- [14] A. Budkowski, U. Steiner and J. Klien, *J. Chem. Phys.* 97 (1992) 5229.
- [15] U. Steiner, J. Klien, E. Eiser, A. Budkowski and J. Fetters, *Science* 258 (1992).
- [16] A. Budkowski, J. Klein, E. Eiser, U. Steiner and L. Fetters, *Macromolecules* (1993) p. 3858.